Thermal Conductivity of Amorphous Polystyrene in Supercritical Carbon Dioxide Studied by Reverse Nonequilibrium Molecular Dynamics Simulations†

Elena A. Algaer,* Mohammad Alaghemandi, Michael C. Böhm, and Florian Müller-Plathe

Eduard-Zintl-Institut für Anorganische und Physikalische Chemie, Technische Universität Darmstadt, Petersenstrasse 20, D-64287 Darmstadt, Germany

Received: February 2, 2009; Revised Manuscript Received: May 20, 2009

The thermal conductivity of amorphous atactic polystyrene (PS) swollen in supercritical carbon dioxide (sc CO_2) has been investigated over wide temperature, pressure, and concentration ranges. Nonequilibrium molecular dynamics simulations with a full atomistic force field have been used to calculate the thermal conductivity of neat PS and sc CO_2 as well as of the binary system at different compositions. An analytical interpolation formula for the thermal conductivity of the binary mixture on the basis of PS and CO_2 data has been obtained. Particular attention has been paid to the implications of the quasi-degeneracy and finite-size effects in the simulated polymer system. It has been found that, in addition to the degrees of freedom per volume, the orientation of the carbon−carbon bonds in the backbone relative to the direction of the temperature gradient is important for the heat transport in PS.

1. Introduction

The thermal conductivity of polymers plays an important role in a number of processing and product applications. Polymers and polymer blends occur in many products and devices. The thermal conductivity (λ) in polymeric thermal insulators, e.g., should be as low as possible. In the encapsulation of electronic devices, however, high λ values are desirable. Moreover, the thermal conductivity is of great importance in the production of polymers. Reliable predictions of the thermal conductivity can lead to improvements in the processing design. As experimental studies over a well-defined pressure (p), temperature (T), and composition range are missing for a number of polymers, computer simulations have become an important tool for the prediction of thermal conductivities in polymer science.

In the past years it has been demonstrated that polymer sorption and swelling processes in supercritical fluids can have advantages in comparison to processes under noncritical conditions. The increasing research activities in this direction are documented in the literature.[1−3] The adoption of carbon dioxide as a supercritical solvent has been guided strongly by ecological reasons. It has been verified experimentally that it is possible to substitute toxic organic solvents by CO_2 without reducing the yield of the process.[4,5]

Polymer processing with supercritical fluids includes purification, impregnation, and fractionation as well as the production of porous foam or powder polymers. Thus it is necessary to investigate the physical properties of polymers swollen in supercritical media. Experimental and simulation techniques have been adopted simultaneously to determine the physical properties of polymers. Despite these activities the behavior of many polymers in supercritical fluids is still not understood completely.

In this paper we have investigated the thermal conductivity of atactic polystyrene (PS) swollen in supercritical CO_2 by reverse nonequilibrium molecular dynamics (RNEMD) simulations.[6] The schematic structure of atactic PS is shown in Figure 1. As experimental λ values for the binary systems have not been reported, we have extended our computer simulations to the components PS and CO_2, for which measured data are available.[7,8] The comparison of calculated and experimental thermal conductivities of the components is a prerequisite to quantify the capability of the present theoretical tools. Our strategy offers a second benefit, i.e., the presentation of an analytical interpolation formula to relate the thermal conductivity of the components PS and CO_2 to the thermal conductivity of the binary mixture. Furthermore, we have considered implications of the quasi-degeneracy in multilevel polymer systems.[9,10] The large number in their degrees of freedom usually leads to a manifold of configurations of roughly the same energy that, however, may differ in other physical properties. Such a manifold of configurations within a narrow energy range is denoted as "quasi-degenerate", a descriptor more popular in electronic structure theory; we refer to the detailed discussion in ref 10. In addition to the finite-size effect, this phenomenon might cause error bars in physical quantities that are larger than the error bars due to the statistical nature of the formalism used. In polymers as well as in solid-state systems, e.g., one can have local modifications in the density, in the spatial arrangement of nonbonded neighbor contacts, or in the magnetic ordering that are energetically quasi-degenerate. To come to the present problem, we have found that the orientation of the carbon−carbon bonds in the backbone of PS relative to the direction of the temperature gradient is important for the heat transport in the system. See ref 8, where this behavior has been confirmed in experiments on oriented and unoriented PS samples. Let us summarize: we have analyzed the thermal

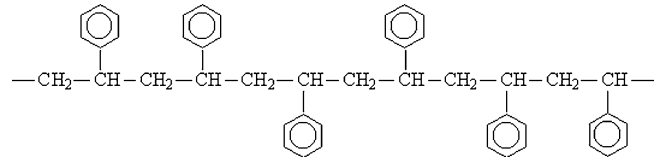

Figure 1. Schematic representation of atactic polystyrene which is characterized by a random distribution of the phenyl rings.

† Part of the "Walter Thiel Festschrift".

* Correspondinga author, e.algaer@theo.chemie.tu-darmstadt.de.

10.1021/jp9009492 CCC: $40.75
Published on Web 07/01/2009

conductivity of PS/CO_2 mixtures as a function of the temperature, pressure, and CO_2 concentration by RNEMD simulations. The computational results of the present approach are detailed in section 4.

2. Reverse Nonequilibrium Molecular Dynamics (RNEMD) Approach

The RNEMD method has been discussed in detail in the literature.[6,11−16] The method was originally proposed for atomic liquids,[6] later extended to molecular fluids and mixtures,[15] and recently modified and tested on polymers.[12] This method allows to calculate transport properties such as the thermal conductivity,[6] the shear viscosity,[13] and the Soret coefficient.[14,16] Other simulation schemes in connection with MD have been suggested quite recently.[17,18] In the second reference the role of anharmonicity on the thermal conductivity has been quantified. The present authors have considered this question in connection with the same RNEMD scheme as adopted in the manuscript in hand.[19]

The RNEMD method for the calculation of transport coefficients is based on the reversal of the experimental cause-and-effect picture. The main idea of the method is to impose a heat flux onto the simulation system as the primary perturbation. Energy is continuously transferred from one region of the system, the so-called "cold" region, to another one, the "hot" region. The direction chosen for the energy transfer, of course, is artificial. We assume that the two regions are separated in the z direction. The total energy of the system is conserved by the transfer process sketched. In the steady state, the same amount of energy per time and area flows from the "hot" to "cold" region by heat conduction. The inverse of the temperature gradient $\langle dT/dz \rangle$ in the intervening region is directly proportional to λ. From the known imposed energy flux j_z and the calculated $\langle dT/dz \rangle$, the thermal conductivity λ can be determined by the relation $\lambda = -j_z/\langle dT/dz \rangle$ assuming the validity of a linear response. In contrast to low-dimensional solids,[20] deviations from Fourier's law are not expected in soft materials.

The artificial energy transfer is generated by exchanging the velocity vectors of the hottest (fastest) atom in the "cold" region and the coldest (slowest) atom in the "hot" region. By the velocity exchange, energy is transferred from the "cold" to the "hot" region. The average energy flux in the steady state can be written as

$$j_z = \frac{1}{2tA} \sum_{\text{transfers}} \frac{m}{2}(v_{\text{hot}}{}^2 - v_{\text{cold}}{}^2) \qquad (1)$$

where t is the simulation time, A is the cross sectional area of the simulation box perpendicular to the flow direction z, and v_{hot} and v_{cold} are the velocities of the hot and cold atoms of identical mass m. The factor 2 arises from the periodicity of the simulation cell in the RNEMD formalism.

At the end of theoretical section we want to emphasize that the work at hand does not intend to give a microscopic picture of the transfer mechanism relevant for the system chosen. A discrimination between vibration-driven and collision-induced transfer channels is a topic of our new paper on PS and PS/CO_2 mixtures.[21] The present data have been prepared to discuss qualitatively differences between the two components, to demonstrate the validity of a simple interpolation scheme, and to verify the confidence limits of the tools adopted.

3. Computational Details

All molecular dynamics simulations have been carried out with the YASP package,[22,23] which uses the leapfrog algorithm and orthorhombic periodic boundary conditions. Temperatures and densities have been chosen at conditions, where experimental information for the components is most abundant. The Berendsen method[24] has been employed to perform simulations at constant temperature. The intramolecular force field contains harmonic bond stretching, harmonic angle bending, and periodic cosine-type torsional potentials. The nonbonded potential includes Lennard-Jones terms with Lorentz−Berthelot mixing rules[25] for unlike interactions as well as electrostatic interactions that are mapped by partial atomic charges. The latter were treated using the reaction-field method with a relative permittivity of 2.5. For details of the functional form of the force field, see ref 26. Nonbonded interactions were evaluated from a Verlet neighbor list, which was updated every 15 timesteps (of 0.001 ps length) using a link-cell method.

A flexible full atomistic model has been used for the present simulations. The force constants for PS have been reported previously for a rigid bond model.[26] The constants for the harmonic bond stretching forces (C(aliphatic)−C(aliphatic), 259780 kJ mol^{-1} nm^{-2}; C(aliphatic)−C(aromatic), 265646 kJ mol^{-1} nm^{-2}; C(aromatic)−C(aromatic), 393022 kJ mol^{-1} nm^{-2}; C−H(aliphatic), 200000 kJ mol^{-1} nm^{-2}; C−H(aromatic), 200000 kJ mol^{-1} nm^{-2}) have been adopted from other work.[12,27] Potential parameters and atomic charges for a flexible full atomistic model of carbon dioxide have been evaluated by Harris and Yung.[28] These authors have adjusted the parameters to reproduce the vapor−liquid coexistence curve and critical properties of carbon dioxide. These parameters have also been used to obtain transport properties, such as the self-diffusion coefficient of carbon dioxide in a supercritical state. It has been shown that the model of Harris and Yung reproduces the transport properties of CO_2 quite well.[29]

The molecular dynamics simulations have been performed at constant temperature and pressure. For the Berendsen thermostat a coupling time τ_T of 0.2 ps and for the barostat a coupling time τ_P of 2 ps have been used. τ_T and τ_P have been sufficient to keep the measured average temperature within 1 K from the target temperature and the measured average pressure within 1 kPa from the target pressure. It has been checked that different choices of τ_T and τ_P did not change the thermal conductivity. In the RNEMD runs, the simulation box was divided into 20 slabs in the direction of the heat flux. Atom velocities were exchanged every 0.5 ps.[11,12] It has been checked that, at this exchange period, the thermal conductivity converges. A nonequilibrium run typically covered 7 ns, the last 1 ns has been used for the production.

An atactic polystyrene chain of 300 monomers with random tacticity of the phenyl rings has been generated in vacuum. In order to check the dependence of the thermal conductivity, several additional simulations with chain length of 100 and 600 monomers have been performed. The thermal conductivity of all samples has been found to be the same within the error bars. Due to the prohibitive computational effort we had to restrict the present simulations to the length of 300 monomers. The size seems to be realistic in order to allow for a comparison with experimental polymers. The discussion of scaling relations as a function of the polymer length is not the topic of the present contribution. We refer to detailed studies where this problem has been considered in detail.[30] The initial polymer conformations have been obtained via pivot Monte Carlo calculations[31] of a single polymer chain in vacuum with a bond-based interaction cutoff to generate a meltlike structure. The interaction cutoff of seven bonds has been chosen on the basis of the persistence length of PS. This chain has been inserted into the

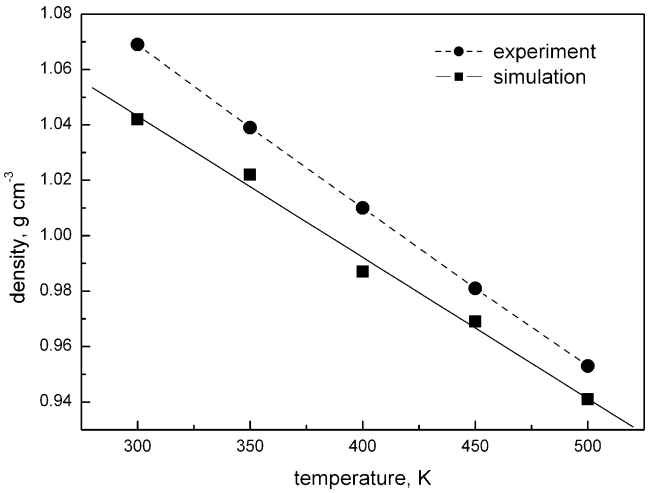

Figure 2. Density of neat PS at 101.3 kPa as obtained by experiment and by simulations.

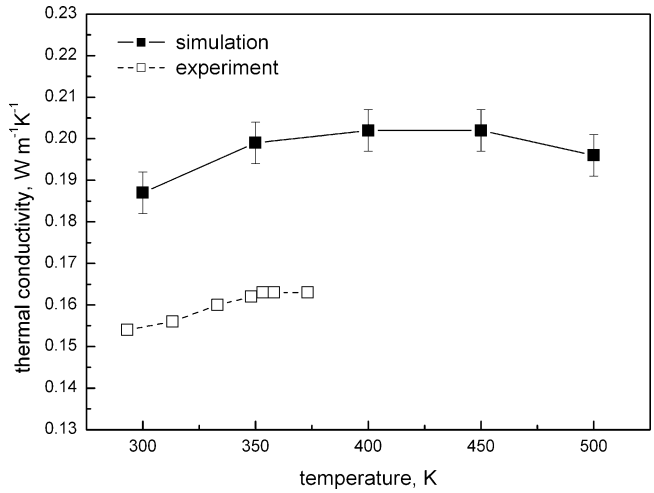

Figure 3. Thermal conductivity of polystyrene versus temperature at 101.3 kPa obtained in experiment and by simulations.

periodic simulation cell. Molecular dynamics simulations with a soft-core potential have been employed to prevent overlaps and to remove possible entanglements and concatenations. Then the system has been equilibrated for 10 ns by equilibrium MD at constant pressure and temperature. After equilibration we have got a cubic simulation box of PS with a density of 1.042 g/cm^3.

A single amorphous atactic polystyrene chain of 300 monomers has been used in all simulations. The following systems have been investigated: neat PS, neat CO_2, and mixtures of PS with different concentrations of CO_2 at supercritical conditions. Simulations have been performed in a temperature range between 350 and 500 K, and for pressures between 101.3 kPa and 60 MPa. Both the temperature and pressure range considered have been employed in experimental studies of the components.[3,32] The concentration of carbon dioxide in the mixture has been varied from 10 to 30 mass %. Four different mixtures with a total number of 79, 125, 177, and 304 CO_2 molecules added to a single PS molecule have been simulated. The binary systems generated by this choice contain 10, 15, 20, and 30 mass % of CO_2.

4. Results and Discussion

4.1. Thermal Conductivity of Neat Polystyrene. The thermal conductivity of neat PS has been calculated in order to compare simulation and experimental results. As validation of the model, we tried to match the simulated density (ρ) of polystyrene at $T = 300$ K and $p = 101.3$ kPa to the experimental one. The density value simulated amounts to 1.042 g/cm^3. Since the simulation has been carried out using orthorhombic periodic boundary conditions the density of simulated PS is defined as mass of a single PS chain divided by the box volume. The experimental density of polystyrene depends both on the structure (syndiotactic or atactic) and on the molecular weight; it varies from 1.032 to 1.069 g/cm^3 at 300 K and 101.3 kPa.[33] The temperature dependence of the simulated and experimental density of neat PS is presented in Figure 2.

As one can see, experiment and simulations agree insofar that the density is reduced linearly with increasing temperature. The calculated densities are however smaller than the measured ones. This might be caused by the fact that the molecular weight of PS in the simulation (~3000 g/mol) is smaller than that obtained by experiment (80000−400000 g/mol).[34]

The calculated thermal conductivity of PS at 300 K and 101.3 kPa amounts to (0.187 ± 0.005) W m^{-1} K^{-1}, while the experimental one at the same temperature and pressure is 0.156 W m^{-1} K^{-1}.[8] We first note that the agreement is quite good. The remaining deviation is of a typical order. The uncertainties of all simulations are defined as a standard deviation from the average in the last 1 ns of production run of the simulation. On the basis of the previous simulation studies in our group[12] we suggest—in addition to the errors caused by the potential—the following explanation for this difference between the present classical simulation data and experiment. The combination "full atomistic model" and "classical MD simulations" guarantees that all spatial degrees of freedom can store energy. The dynamics of the atoms is not restricted by energy quantization. In a more realistic quantum approach all degrees of freedom would have to be described by nuclear fluctuations in the vibrational ground state or—for soft modes—in excited states. The stiff degrees of freedom, however, cannot be excited thermally as their vibrational energy (in wavenumber units) is found between 1000 and 2500 cm^{-1}, whereas the thermal energy at room temperature amounts to 207 cm^{-1}. Hence, these modes are not accessible for the transport of energy in the quantum limit realized experimentally. This distinction between a classical model and experiment may explain the remaining overestimation of λ. The improvement of RNEMD results due to quantum correction have been commented on in our recent simulation study on carbon nanotubes.[35] For the thermal conductivity of polyamide-6,6, it has been reported that the best agreement with experiment occurs for a fully bond-constrained united-atom model.[12] Even under the neglect of error compensations we have found that the flexible atomistic model chosen leads to a sufficient agreement between experiment and simulation. This might indicate that the dominant mechanisms of the thermal transport in polyamide-6,6 and polystyrene differ. In polystyrene the most important heat transfer channel is along the backbone.[36] Heat transfer through phenyl rings (by collisions) is less important. As mentioned above this discrimination between phonon-assisted and collision-induced thermal conductivities will be considered in our next contribution. It has been observed and reported before for syndiotactic PS that not only the number of degrees of freedom is important but also their spatial location.[36]

The next benchmark chosen has been the temperature dependence of the thermal conductivity of neat PS. The simulation and experimental results over a wide temperature range are plotted in Figure 3. The calculated thermal conductivity grows at lower temperatures and converges to a constant

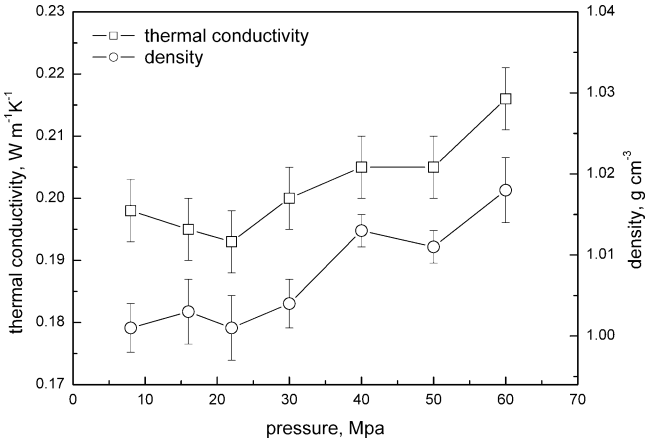

Figure 4. Thermal conductivity and density of polystyrene versus pressure at 400 K.

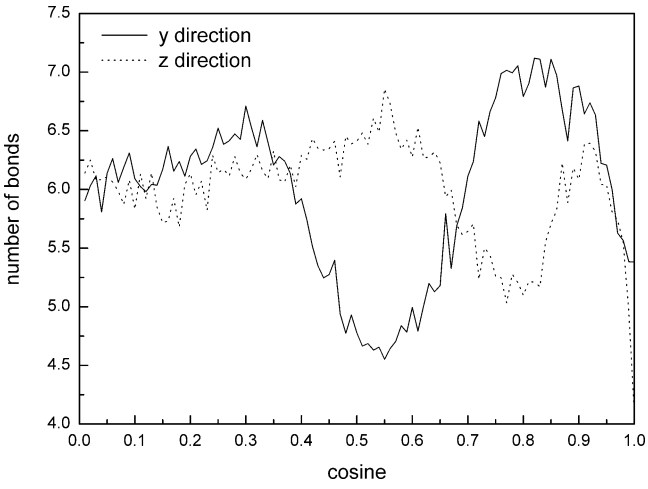

Figure 5. Orientation of C−C bonds in the backbone.

value between 400 and 450 K. This trend is in line with experimental results showing a constant plateau between 350 and 380 K.[8] In Figure 3 we see that the simulated λ is again reduced for $T > 450$ K. Due to the error bars of the simulations, this statement should be used only with care.

The pressure dependence of the thermal conductivity and density are shown in Figure 4. As could be expected a priori, density and thermal conductivity are both enhanced with increasing pressure. Experimental information is not available.

In a large number of simulations we have found that the thermal conductivity of PS strongly depends on the number and orientation of C−C bonds in the backbone relative to the direction of the temperature gradient (and the collinear heat flux). In order to demonstrate this effect, we have calculated the thermal conductivity of the same polystyrene sample in two perpendicular directions, i.e., *y* and *z*. Remember, however, that the simulation cell as well as the pressure is isotropic. Differences in λ in the two directions are a manifestation of the above-mentioned quasi-degeneracy as well as finite-size effects. The present RNEMD simulations into the two perpendicular directions lead to thermal conductivities of 0.213 and 0.179 W m^{-1} K^{-1}. Then we have calculated the direction cosine of all backbone C−C bonds relative to the direction of the heat transport. In other words we have calculated the orientation of C−C bonds in the backbone. The results are presented in Figure 5.

As one can see, the number of backbone bonds oriented into the *y* direction is larger than the number of bonds oriented into

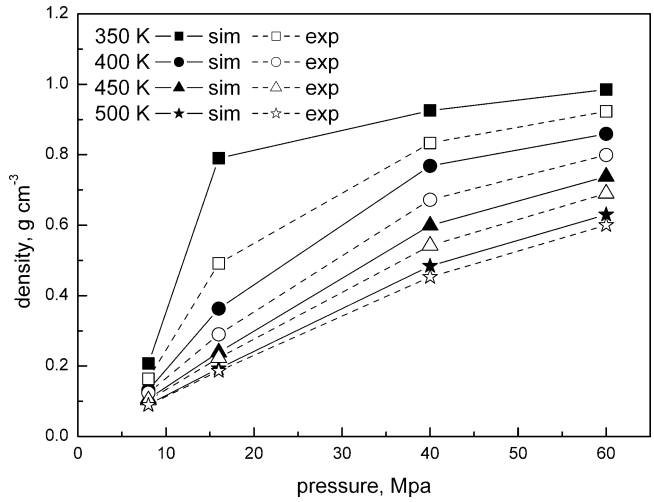

Figure 6. Simulated and experimental[37] densities of CO_2 under supercritical conditions. The uncertainties in the simulated densities are smaller than the size of the symbols.

z direction. The implications of this difference can be seen in the two λ values, the thermal conductivity is larger in the *y* direction and smaller in the *z* direction.

It has been found in both experiments and the present simulations that a preferred orientation of the backbone of the polymer in the direction of the temperature gradient may lead to an enhancement in the thermal conductivity.[8,12] It proves that the thermal transport in polymers is faster when it progresses along the chain via phonons than by means of lateral collisions. This topic will be discussed in more detail in connection with RNEMD simulations on stretched and nonstretched PS.[21] Here, we should mention that polymer systems are so-called multilevel systems with a manifold of quasi-degenerate configurations with non-negligible differences in the nature of local nonbonded contacts. This phenomenon as well as the finite-size effect in the polystyrene system leads to the thermal conductivity values reflecting differences in the local geometric arrangements which are often predetermined by the initial configuration chosen.[9,10] To calculate the error bars of the simulations, eight different initial configurations of PS system have been investigated by simulation runs. The average thermal conductivity at 400 K and at 40 MPa amounts to (0.205 ± 0.012) W m^{-1} K^{-1}. Thus we have to accept an additional error of 6% in the thermal conductivity caused by the above influence factor, structural difference of microstructures with almost identical energies.

4.2. Simulation of Neat Supercritical Carbon Dioxide. Carbon dioxide has been simulated under supercritical conditions to check the accuracy of the calculated properties in this limit. As mentioned in section 3, the force constants required have been determined by Harris and Yung[28] with the aim to calculate supercritical properties of carbon dioxide with high accuracy. We have calculated the density and the thermal conductivity of CO_2 under supercritical conditions over a wide pressure and temperature range. The simulated and experimentally estimated[37] densities of CO_2 versus pressure for different temperatures are plotted in Figure 6. The density increases with the pressure. In the studied temperature interval between 350 and 500 K the density at a given pressure is reduced with increasing temperature.

The comparison with the "experimental" densities derived via an equation of state[37] indicates that the simulated carbon dioxide densities in Figure 6 at different pressures are typical for supercritical conditions. It is obvious that problems caused by the quasi-degeneracy and finite-size effects as emphasized

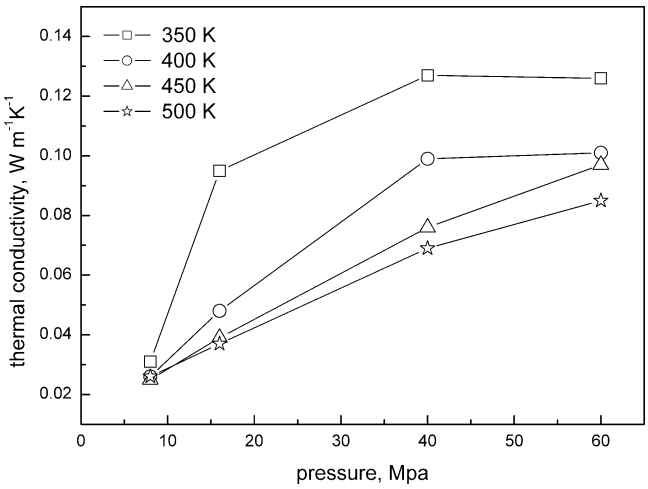

Figure 7. Thermal conductivity of CO_2 at supercritical conditions versus pressure at different temperatures. The uncertainties of the simulated thermal conductivity are smaller than the size of the symbols.

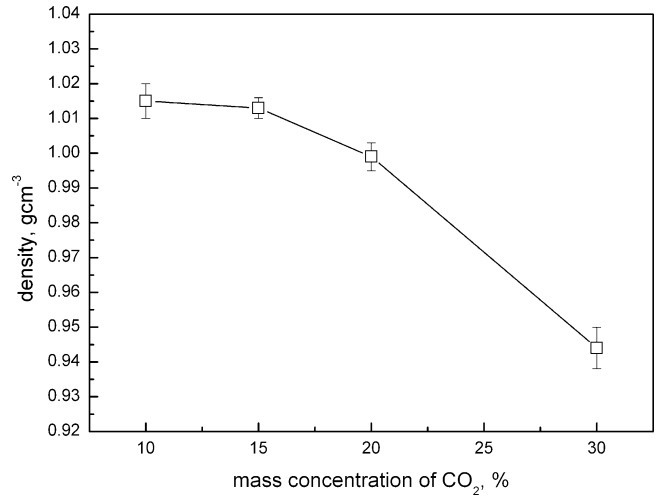

Figure 8. Density of the binary mixture versus CO_2 concentration in mass % at 400 K and 16 MPa.

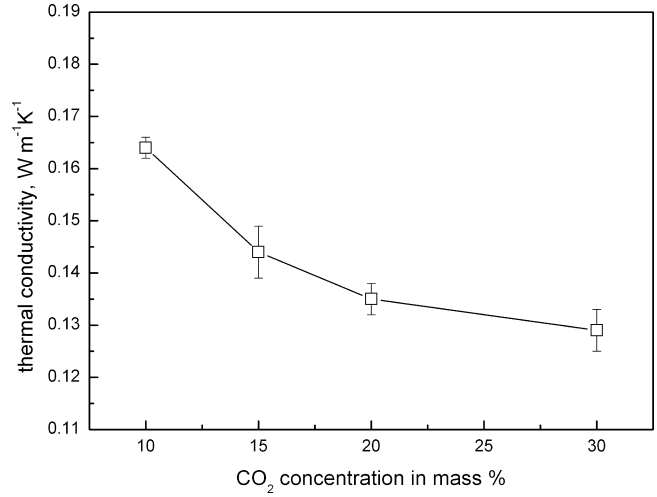

Figure 9. Thermal conductivity of the binary mixture versus mass concentration of CO_2 in % at 400 K and 16 MPa.

for PS do not occur for systems with a simple geometric structure such as CO_2. Before commenting on the thermal conductivity data of CO_2, we want to mention that the density of CO_2 is smaller than the density of PS. This difference is particularly large for not too high pressures. In order to understand the thermal conductivity values of the binary mixtures, we should mention that in classical simulations, density enhancement implies an enhancement in the degrees of freedom per volume element and thus more transport channels for the heat.[12]

The pressure dependence of the thermal conductivity of supercritical CO_2 is displayed in Figure 7. The error bar in the simulations of CO_2 is much smaller than that in the PS case. It is clear that this difference is an outcome of the fact that the multilevel problem is restricted to polymers. Correlation with Figure 6 indicates that the thermal conductivity and density profiles are of similar shape; see above. The same analytical shape has been observed for the measured thermal conductivity of CO_2.[38] In analogy to the density, the thermal conductivity grows with the pressure and decreases with increasing temperature. The comparison of the simulated data for PS and CO_2, see Figures 4 and 7, demonstrates that both materials coincide in the qualitative pressure dependence of the thermal conductivity. However, they differ in their temperature dependence. In PS the thermal conductivity increases first with increasing temperature and then it reaches the plateau before it drops again; please remember the uncertainties in the PS simulations. The thermal conductivity of CO_2 is continuously reduced as a function of temperature. The calculated thermal conductivity of CO_2 under supercritical conditions will be used below to evaluate an empirical thermal conductivity formula for the mixture on the basis of the neat PS and CO_2 data.

4.3. Thermal Conductivity of Mixtures of Polystyrene and Supercritical Carbon Dioxide. The polystyrene chain has been mixed with different concentrations (10, 15, 20, and 30 mass %) of CO_2. In Figure 8 we present the density of the binary mixtures at $T = 400$ K and $p = 16$ MPa as a function of the CO_2 concentration obtained from an equilibrium calculation. The density decreases with an enhanced CO_2 concentration. In consideration of the above discussion of the particle densities of CO_2 and PS, this density reduction has been expected. It is a manifestation of the fact that the number of chemical bonds per atom in PS exceeds the average number of bonds in CO_2.

The binary mixtures considered have been equilibrated for 6 ns. After this period RNEMD runs of 7 ns have been performed. The last 1 ns has been used for the calculation of the thermal conductivity of the systems. The thermal conductivity of the binary mixture as a function of the CO_2 concentration is shown in Figure 9. The observed reduction of the thermal conductivity with increasing CO_2 concentration could be expected a priori on the basis of the thermal conductivity values of neat PS and CO_2.

The pressure dependence of the thermal conductivity of the four mixtures is shown in Figure 10. The thermal conductivity of the mixtures slightly increases with increasing pressure and decreases with increasing mass concentration of CO_2. A similar modification of λ as a function of pressure has been observed for the separate components. The data in the figure clearly emphasize that the density enhancement with increasing pressure makes the heat transfer more efficient. Now let us consider the four curves in Figure 10 in more detail. Due to the higher compressibility of CO_2 relative to PS, we expect that the pressure dependence of the thermal conductivity is enhanced with increasing CO_2 concentration. With the exception of the 15% curve, this effect seems to be realized in Figure 10. We cannot rule out that the shape of this 15% curve is a result of the error bars of the simulations. For the small CO_2 concentrations considered, the above enhancement, however, is rather small.

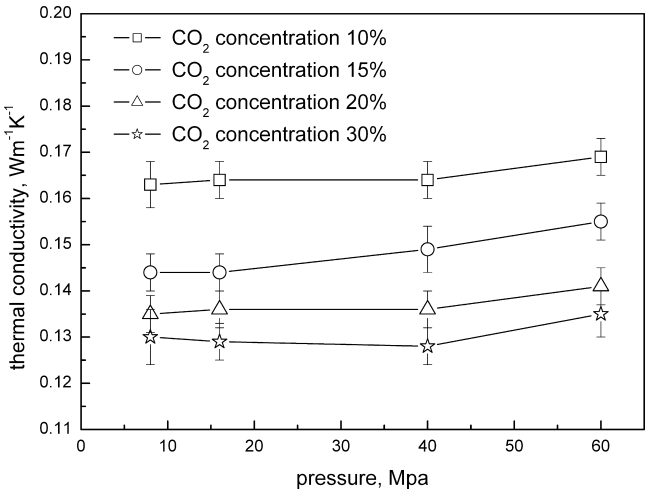

Figure 10. Thermal conductivity of binary mixtures versus pressure for different mass concentrations of CO_2 in % at 400 K.

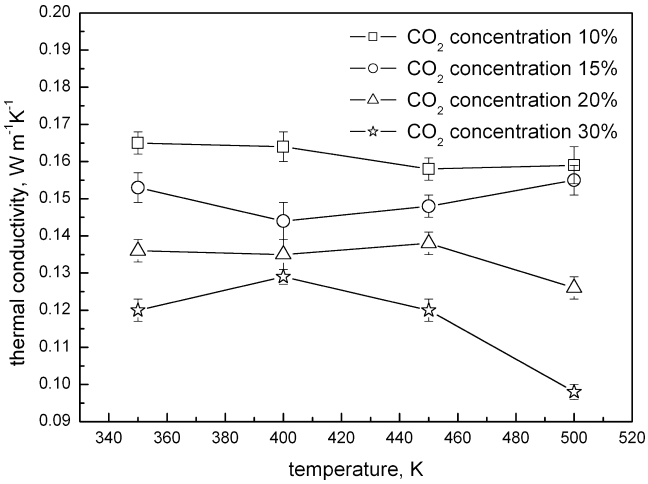

Figure 11. Thermal conductivity of binary mixtures versus temperature for different mass concentrations of CO_2 in % at 16 MPa.

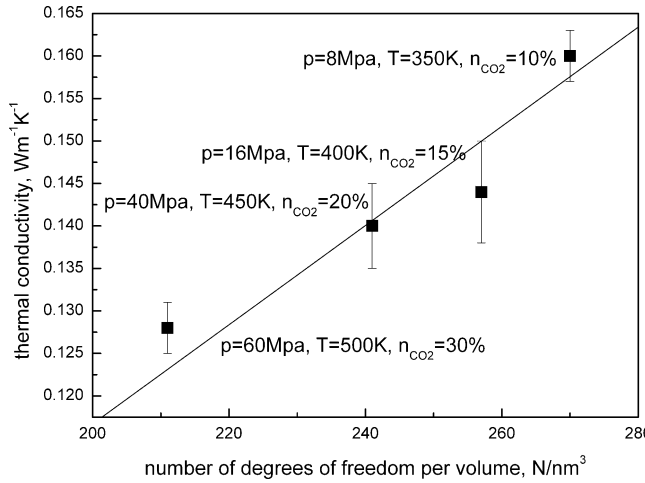

Figure 12. Thermal conductivity of binary PS/CO_2 admixtures as a function of the degrees of freedom per unit volume encountered in the system.

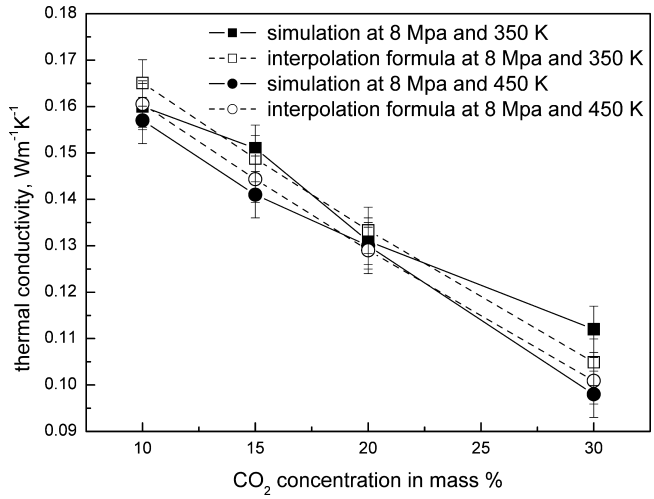

Figure 13. Thermal conductivity of the binary mixtures as a function of CO_2 mass concentration derived by RNEMD simulations of the binary system and estimated via the interpolation.

In Figure 11 we display the temperature dependence of the thermal conductivity for the four different binary systems. The thermal conductivity curves show two expected trends. (a) The thermal conductivity is reduced with an increasing amount of CO_2; again we refer to the above analysis. (b) The curve shape of the thermal conductivity at high temperatures (i.e., $T > 450$ K) of the two mixtures with the lowest CO_2 admixtures differs from the behavior predicted for the materials with the two highest CO_2 concentrations. For the two latter mixtures the thermal conductivity is reduced with increasing temperature while it is enhanced or remains constant for the two samples with small CO_2 admixtures. This switch in the temperature profile reflects differences in the temperature dependence of the thermal conductivity for the two components; see again Figures 3 and 7. For PS we have a temperature window where the thermal conductivity is an increasing function of temperature while the CO_2 thermal conductivity is always reduced with increasing temperature. With an enhanced amount of CO_2 this negative gradient becomes more dominant.

As it has been reported in previous work[12,36] and mentioned above, the number of degrees of freedom is a decisive quantity for the thermal transport. We have calculated the thermal conductivity of PS as a function of the number of degrees of freedom per volume. The results of the calculations are presented in Figure 12 for a selection of the systems investigated. The thermal conductivity increases with an enhanced number of degrees of freedom. The line in Figure 12 results from a linear fit of the simulated data under the boundary condition to cross the origin (0,0). This choice reflects the fact that an energy transport is not possible in the absence of any degrees of freedom.

The rather large scattering in Figure 12 clearly indicates that the number of the degrees of freedom, i.e., the number of atoms, is only one parameter influencing the thermal conductivity. In the present work we have shown that the degrees of freedom are not equivalent. Recall the decisive role of the orientation of the bonds in the polystyrene backbone. Up to now the influence of the temperature on this correlation has not been commented on. The different temperature dependence of λ and the density clearly indicate that the correlation between λ and number in the degrees of freedom is strictly valid only for a constant temperature. However, it seems that this temperature effect leads to minor modifications only.

On the basis of the thermal conductivities of the neat PS and CO_2 systems, we have obtained an empirical interpolation formula for λ of the mixture as a function of the concentration of CO_2, pressure, and temperature. The data for the two components at different conditions are summarized in Table 1.

TABLE 1: Thermal Conductivities of Neat PS and Neat CO_2 at Different Temperatures and Pressures, Experimental Values[38] in Parentheses

p, MPa	T, K	λ of PS, W m^{-1} K^{-1}	λ of CO_2, W m^{-1} K^{-1}
8	350	0.191	0.031 (0.028)
	400	0.198	0.026 (0.030)
	450	0.201	0.025 (0.033)
	500	0.197	0.026 (0.036)
16	350	0.189	0.095 (0.056)
	400	0.195	0.048 (0.040)
	450	0.201	0.039 (0.039)
	500	0.198	0.037 (0.040)
40	350	0.201	0.127 (0.097)
	400	0.205	0.099 (0.076)
	450	0.210	0.076 (0.064)
	500	0.206	0.069 (0.059)
60	350	0.205	0.126 (0.115)
	400	0.216	0.101 (0.095)
	450	0.216	0.097 (0.081)
	500	0.208	0.085 (0.074)

The interpolation formula for the thermal conductivity of the binary mixture reads

$$\lambda_{mix}(C_{CO_2}, p, T) = \frac{(1 - C_{CO_2})((1 - C_{CO_2})\lambda_{PS}(p, T) + C_{CO_2}\lambda_{CO_2}(p, T))}{(0.00904 - 0.00002T)p + (0.6228 + 0.0009T)} \quad (2)$$

where C_{CO_2} is the mass fraction of CO_2 in the mixture, T the temperature in Kelvin, and p the pressure in MPa.

The starting thermal conductivity value has been estimated as follows: Assume that the thermal conductivity of the mixture is proportional to λ of the neat components weighted by their mass fraction. In order to determine λ_{mix} with sufficient accuracy, we had to consider the influence of pressure and temperature in the denominator of the interpolation formula. Deviations from the simple additivity are taken into account by a multiplicative constant f_{na} in the numerator. It turned out that f_{na} can be approximated by $(1 - C_{CO_2})$. For $C_{CO_2} \rightarrow 0$ the interpolation scheme reproduces the correct asymptotic limit λ_{PS} but fails to map the boundary $C_{CO_2} \rightarrow 1$. The thermal conductivity of the mixture obtained from this formula differs by less than 10% from the value calculated for the binary system. A comparison of the thermal conductivity as calculated from this formula and from simulations is presented in Figure 13. The interpolated and exactly calculated thermal conductivities coincide within the error bars of the simulation.

Interpolation schemes of the present type might be useful, when the theoretical determination of quantities of a binary system over a large concentration, pressure, and temperature range is intended on the basis of a smaller set of simulation or experimental results.

5. Conclusions

The thermal conductivity λ of amorphous atactic polystyrene swollen in supercritical carbon dioxide has been investigated over a wide temperature, pressure, and concentration range by nonequilibrium molecular dynamics simulations with a full atomistic model for the force field. The data for the binary systems have been supplemented by thermal conductivity values derived for the components PS and CO_2. Neat PS as well as the binary mixtures are so-called multilevel systems characterized by very small energy fluctuations in the presence of larger fluctuations of other physical quantities. Computer simulations of such systems are very time-consuming as it requires a high effort and much experience to reduce the error bars for the quantities studied to an acceptable minimum. The pressure and temperature dependence of the thermal conductivity has been discussed in detail. For the neat components, it has been possible to relate the calculated results to experimental data. Density trends for both PS and CO_2 have reproduced the experimental ones correctly. The thermal conductivity of PS differs from experiment by less than 20%. We have shown that the thermal conductivity of PS is much larger than the thermal conductivity of CO_2. This leads to a reduction of the thermal conductivity of the mixture with an enhanced concentration of CO_2. It has been possible to present an interpolation formula for the thermal conductivity of the binary samples on the basis of λ values for the two components PS and CO_2.

The present RNEMD simulations have reproduced another recent result, i.e., the correlation between the thermal conductivity and the number of C−C bonds in the polymer backbone in the direction of the temperature gradient. In a future article this topic will be analyzed in more detail for PS samples under uniaxial stress. Furthermore, we plan to interpret the results of our computer simulations by microscopic arguments. We intend to identify the participation of the different degrees of freedom in the heat transfer. The data at hand should be accepted as a first step to derive theoretical thermal conductivity values for polymer mixtures and solutions not studied by MD simulations up to now.

Acknowledgment. Financial support of the present work by the Deutsche Forschungsgemeinschaft is gratefully acknowledged.

References and Notes

(1) Chang, S. H.; Park, S. C.; Shim, J. J. *J. Supercrit. Fluids* **1998**, *13*, 113.
(2) Cooper, A. I. *J. Mater. Chem.* **2000**, *10*, 207.
(3) Nikitin, L. N.; Gallyamov, M. O.; Vinokur, R. A.; Nikolaev, A. Y.; Said-Galiyev, E. E.; Khokhlov, A. R.; Jespersen, H. T.; Schaumburg, K. *J. Supercrit. Fluids* **2003**, *27*, 131.
(4) Kendall, J. L.; Canelas, D. A.; Young, J. L.; De Simone, J. M. *Chem. Rev.* **1999**, *99*, 543.
(5) Watkins, J. J.; McCarthy, T. J. *Macromolecules* **1994**, *27*, 4845.
(6) Müller-Plathe, F. *J. Chem. Phys.* **1997**, *106*, 6082.
(7) Gupta, G. P.; Saxena, S. C. *Mol. Phys.* **1970**, *19*, 871.
(8) Pasquino, A. D.; Pilswort, Mn *J. Polym. Sci., Part B: Polym. Lett.* **1964**, *2*, 253.
(9) Binder, K.; Stauffer, D. *Application of the Monte Carlo Method in Statistical Physics*; Springer Verlag: Berlin, Heidelberg, 1987.
(10) Böhm, M. C.; Elsässer, C.; Fähnle, M.; Brandt, E. H. *Chem. Phys.* **1989**, *130*, 65.
(11) Müller-Plathe, F. In *Novel Methods in Soft Matter Simulations*; Kartunnen, M., Vattulainen, I., Lukkarinen, A., Eds.; Lecture Notes in Physics 640; Springer: Heidelberg, Germany, 2004; pp 310.
(12) Lussetti, E.; Terao, T.; Müller-Plathe, F. *J. Phys. Chem. B* **2007**, *111*, 11516.
(13) Müller-Plathe, F. *Phys. Rev. E* **1999**, *59*, 4894.
(14) Zhang, M. M.; Müller-Plathe, F. *J. Chem. Phys.* **2005**, *123*.
(15) Zhang, M. M.; Lussetti, E.; De Souza, L. E. S.; Müller-Plathe, F. *J. Phys. Chem. B* **2005**, *109*, 15060.
(16) Zhang, M.; Müller-Plathe, F. *J. Chem. Phys.* **2006**, *125*.
(17) Henry, A.; Chen, G. *Phys. Rev. Lett.* **2008**, *101*.
(18) Shenogin, S.; Bodapati, A.; Keblinski, P.; McGaughey, A. J. H. *J. Appl. Phys.* **2009**, *105*.
(19) Alaghemandi, F., Leroy, E., Algaer, M. C., Böhm, M. C., Mŭller-Plathe, F. *Phys. Rev. B* **2009**, submitted.
(20) Chang, C. W.; Okawa, D.; Garcia, H.; Majumdar, A.; Zettl, A. *Phys. Rev. Lett.* **2008**, *101*.
(21) Algaer, E., Alaghemandi, M., Böhm, M. C., Mŭller-Plathe, F., 2009.
(22) Müller-Plathe, F. *Comput. Phys. Commun.* **1993**, *78*, 77.
(23) Tarmyshov, K. B.; Müller-Plathe, F. *J. Chem. Inf. Model.* **2005**, *45*, 1943.
(24) Berendsen, H. J. C.; Postma, J. P. M.; van Gunsteren, W. F.; Dinola, A.; Haak, J. R. *J. Chem. Phys.* **1984**, *81*, 3684.
(25) Allen, M. P., Tildesley, D. J. *Computer Simulation of Liquids*; Oxford Science Publisher: Oxford, 1987.

(26) Müller-Plathe, F. *Macromolecules* **1996**, *29*, 4782.
(27) Valavala, P. K.; Odegard, G. M. *Rev. Adv. Mater. Sci.* **2005**, *9*, 34.
(28) Harris, J. G.; Yung, K. H. *J. Phys. Chem.* **1995**, *99*, 12021.
(29) Zhang, Z. G.; Duan, Z. H. *J. Chem. Phys.* **2005**, *122*.
(30) Hansen, D.; Ho, C. C. *J. Polym. Sci., Part A: Gen. Pap.* **1965**, *3*, 659.
(31) Brown, D. *The gmq user manual verision 4*; University of Savoie, 2008.
(32) Wang, W. C. V.; Kramer, E. J.; Sachse, W. H. *J. Polym. Sci., Part B: Polym. Phys.* **1982**, *20*, 1371.
(33) Höcker, H.; Blake, G. J.; Flory, P. J. *Trans. Faraday Soc.* **1971**, *67*, 2251.
(34) Carwille, L. C. K.; Hoge, H. J. *Thermal Conductivity of Polystyrene: Selected Values*; Pioneering Research Division, U.S. Army Natick Laboratories, 1966.
(35) Alaghemandi, M.; Algaer, E.; Böhm, M. C.; Müller-Plathe, F. *Nanotechnology* **2009**, *20*.
(36) Rossinsky, E.; Müller-Plathe, F. *J. Chem. Phys.* 2009.
(37) Span, R.; Wagner, W. *J. Phys. Chem. Ref. Data* **1996**, *25*, 1509.
(38) Vesovic, V.; Wakeham, W. A.; Olchowy, G. A.; Sengers, J. V.; Watson, J. T. R.; Millat, J. *J. Phys. Chem. Ref. Data* **1990**, *19*, 763.

JP9009492